

CHAPTER 1

DEVELOPMENT OF RADIATION-PROTECTIVE COATINGS
BASED ON EPOXY COMPOSITES FOR MATERIALS OF
ELECTRONIC EQUIPMENT

CHAPTER 1

ABSTRACT

The basics of the theory of electron energy loss when passing through a composite material are presented. This made it possible to explain the influence of the metal filler on the amount of such losses. Dependences of the electron concentration, specific conductivity, and Hall EMF on the induction of external magnetic field for the n-Si and n-Ge single crystals, irradiated by the fast electrons, coated with a layer of ED-20 epoxy resin, were obtained. The composite layer was without fillers and with iron and aluminum powders as fillers. The presence of such a coating layer increases the radiation resistance of n-Si and n-Ge single crystals. Silicon and germanium single crystals coated with epoxy composite with iron powder filler have the highest radiation resistance. Obtained dependences of the Hall EMF on the induction of magnetic field for the investigated n-Si and n-Ge samples are linear. Only the silicon and germanium single crystals coated with epoxy with iron powder filler exhibit slight deviation from linearity at magnetic fields below 0.3 T. Residual magnetization, which induced the additional EMF Hall, was detected for the germanium and silicon single crystals, coated with a layer of epoxy resin with the iron powder filler. The presence of residual magnetization of the iron powder filler and the corresponding induced additional Hall EMF can be of practical importance in the development of energy storage systems based on irradiated n-Ge and n-Si single crystals coated with a layer of epoxy resin with the iron powder filler.

The chapter for a wide range of specialists with the radiation physics of solids is designed. It will be useful also for graduate students and students of physical and physical-technical specialties.

KEYWORDS

Epoxy composite coatings, Hall effect, radiation defects, radiation resistance, magnetic sensitivity, silicon and germanium single crystals, radiation losses, metal powder fillers.

Currently, there is a growing need for new materials with specific properties or known materials with improved properties [1–6]. Advances in some fields of technology are largely determined

by the ability of such materials to function in extreme conditions, such as elevated levels of radiation, temperature, chemical activity, mechanical and tribotic loads. The modern development of the nuclear industry, nuclear energy, military, and space technology is in dire need of the development of a new generation of electronic equipment based on these materials. The design of such devices is relevant to ensure the safety of work at nuclear and space plants, the disposal of nuclear waste, and work in radioactively contaminated areas. In addition, high-radiation physical experiments performed on charged particle accelerators at CERN require semiconductor devices capable of providing long-term dosimetric control in the internal tracks of nuclear installations. Devices with such performance are not available worldwide and cannot be designed using traditional semiconductor materials technologies, such as monocrystalline silicon and germanium technologies. Also, the use of already known materials and products to solve such problems creates the need not only to assess their radiation resistance in order to determine the limits of applicability but also the ability to use radiation as a technological tool to improve the properties of these materials. The problem of protection of semiconductor electronics elements from radiation can be solved by applying local radiation protection, the essence of which is to use special coatings that are directly applied to the surface of such elements. Promising in this direction is the development and application of polymer composite coatings based on epoxy resins, which have a number of advantages over other reactive polymers due to high manufacturability, adhesive strength, hardness, wear resistance, corrosion resistance, and resistance to rapidly changing temperature fields. Also, such coatings are lighter and cheaper compared to metal cases. Therefore, the development of a set of physical-mechanical and operational properties of epoxy composites and, accordingly, obtaining protective coatings for silicon and germanium single crystals from the aggressive action of radiation, environment, and other high-energy physical fields will allow creating of fundamentally new elements and devices of extreme electronics.

1.1 TOTAL ENERGY LOSSES OF ELECTRONS WHEN PASSING THROUGH THE POLYMER COMPOSITE

During the operation of spacecraft in the Earth's radiation belts, materials located on the outer surface area exposed to electron flows with a wide energy spectrum. Thermalizing in dielectric materials, these particles are able to create an uncompensated electric charge, i.e. to cause radiation electrification, which can significantly change the electrophysical properties of dielectrics [7]. Therefore, one of the main reasons that lead to the failure of electronic and electrical equipment of the spacecraft is the electrical breakdown of dielectrics. In the orbits of spacecraft, where there are intense flows of high-energy electrons, the absorbed dose of radiation inside is mainly determined not by electrons but by their radiation. It is known that in a geostationary orbit the absorbed radiation dose from hard electromagnetic radiation under radiation protection in 11 mm aluminum is more than two thousand times higher than the radiation dose from the electrons that generate this radiation. For polymers, this problem is less relevant, as they weakly generate

inhibitory X-rays caused by exposure to the protective material of high-energy corpuscular radiation. In addition, the polymeric materials have a lower density, which reduces the weight of the protective material at the initial level of protection. To use a new polymer composite in space, it is necessary to mathematically model the effect of electron radiation on it. In [7], a polymer composite (PC) synthesized on the basis of impact-resistant polystyrene and organosiloxane methylpolysiloxane xerogel filler (MPS) was selected. The elemental composition of the PC is presented in **Table 1.1**. It was previously found that this composition is optimal for use in space. The temperature interval of polystyrene composite operation is from +160 °C to –170 °C, it is resistant to VUV radiation and atomic oxygen.

● **Table 1.1** Elemental composition of the PC

The content of the MPS, wt. %	The content of elements in the composite, wt. %			
	Si	O	H	C
60	24	17.633	6.750	51.617

Consider a polymeric, completely amorphous composite material with a density $\rho = 1.159 \text{ g/cm}^3$. To study the ionization energy losses during the passage of electrons through the investigated polymer composite material, let's use the formula [8]:

$$\left(-\frac{dE}{dx} \right)_{col} = K \rho \frac{Z}{A} \frac{1}{2\beta^2} \left[\ln \left(\frac{m_e c^2 E_k}{I^2} \frac{\beta^2}{2(1-\beta^2)} \right) - \frac{(2\sqrt{1-\beta^2} - 1 + \beta^2) \ln 2 + 1 - \beta^2 + \frac{1}{8}(1 - \sqrt{1-\beta^2})^2}{\beta^2} \right], \quad (1.1)$$

where $K = 4\pi \cdot r_e^2 m_e c^2 N_A = 0.307 \text{ MeV/g/cm}^2$;

$m_e c^2 = 0.511 \text{ MeV}$ – the rest energy of the electron;

$r_e = e^2 / m_e c^2 = 2.8 \cdot 10^{-13} \text{ cm}$ – classical electron radius;

$N_A = 6 \cdot 10^{23} \text{ 1/mol}$;

ρ – the density of the substance;

I – the average ionization potential of the atom of the substance of the medium;

$\beta = \sqrt{1 - \frac{(m_e c^2)^2}{(m_e c^2 + E_k)^2}}$ – Lorentz factor of an electron with kinetic energy E_k .

The studied composite material consists of atoms of different grades, each of which will contribute to the ionization energy loss of electrons. Then the formula will be:

$$\left(-\frac{dE}{dx}\right)_{cal} = \sum_i \left(-\frac{dE}{dx}\right)_i, \quad (1.2)$$

where $(-dE/dx)_i$ is the density and contribution of the i -th element in the complex substance and the ionization losses of the electron.

Rewrite expression (1.1) in a more convenient form for analysis:

$$\left(-\frac{dE}{dx}\right)_{cal} = \rho \frac{Z}{A} F(E_k, I), \quad (1.3)$$

$$F(E_k, I) = \frac{K}{2\beta^2} \left[\ln \left(\frac{m_e c^2 E_k}{I^2} \frac{\beta^2}{2(1-\beta^2)} \right) - (2\sqrt{1-\beta^2} - 1 + \beta^2) \ln 2 + \left[1 - \beta^2 + \frac{1}{8} (1 - \sqrt{1-\beta^2})^2 \right] \right]. \quad (1.4)$$

In this case, the contribution of each element to the total ionization losses is as follows:

$$\left(-\frac{dE}{dx}\right)_{cal}^C = \rho_C \frac{Z_C}{A_C} F(E_k, I_C), \quad (1.5a)$$

$$\left(-\frac{dE}{dx}\right)_{cal}^{Si} = \rho_{Si} \frac{Z_{Si}}{A_{Si}} F(E_k, I_{Si}), \quad (1.5b)$$

$$\left(-\frac{dE}{dx}\right)_{cal}^O = \rho_O \frac{Z_O}{A_O} F(E_k, I_O), \quad (1.5c)$$

$$\left(-\frac{dE}{dx}\right)_{cal}^H = \rho_H \frac{Z_H}{A_H} F(E_k, I_H). \quad (1.5d)$$

The average ionization potentials of atoms have the following values:

$$I_C \approx 785V, I_{Si} \approx 1735V, I_O \approx 955, I_H \approx 19.25V. \quad (1.6)$$

Given (1.5a–c), the ionization energy loss of electrons in the studied composite material is written in the form:

$$\left(-\frac{dE}{dx}\right)_{col} = \rho_C \frac{Z_C}{A_C} F(E_k, I_C) + \rho_{Si} \frac{Z_{Si}}{A_{Si}} F(E_k, I_{Si}) + \rho_O \frac{Z_O}{A_O} F(E_k, I_O) + \rho_H \frac{Z_H}{A_H} F(E_k, I_H). \quad (1.7)$$

Fig. 1.1 presents the curves constructed on the basis of expressions (1.3–1.7), showing the total ionization losses of electrons in the polymer composite (thicker curve) and the separate contribution of each chemical element of the composite to the ionization losses. From **Fig. 1.1** it follows that a greater contribution to the ionization losses is made by the carbon component while taking into account the low density of the composite, energy losses are quite high.

In addition to ionization losses, there are also radiation energy losses of electrons when passing through the investigated polymer composite material. Radiation energy losses of the electron in the matter are equal:

$$\left(-\frac{dE}{dx}\right)_{rad} = p \frac{Z^2 K \alpha \varepsilon}{A 4\pi m} G(E_k), \quad (1.8)$$

where $F(x) = \int_0^x \frac{\ln(1+y)}{y} dy$; $\varepsilon = E_k + m_e c^2$ – total electron energy; p – electron momentum.

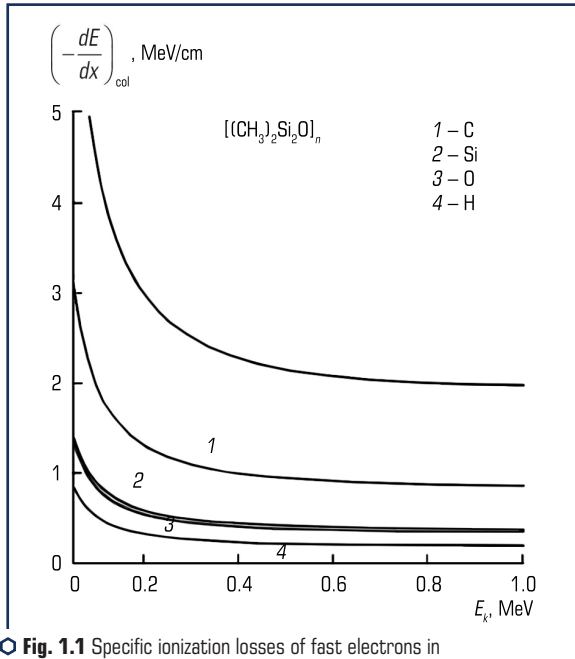


Fig. 1.1 Specific ionization losses of fast electrons in the polymer composite

$$G(E_k) = \frac{K\alpha}{4\pi} \frac{\varepsilon}{m} \left[\frac{12\varepsilon^2 + 4m_e^2 c^4}{3\varepsilon p} \ln\left(\frac{\varepsilon + p}{m_e c^2}\right) - \frac{(8\varepsilon + 6p)m_e^2 c^4}{3\varepsilon p^2} \left(\ln\left(\frac{\varepsilon + p}{m_e c^2}\right)\right)^2 - \right. \\ \left. - \frac{4}{3} + \frac{2m_e^2 c^4}{\varepsilon p} F\left(\frac{2p(\varepsilon + p)}{m_e^2 c^4}\right) \right]. \quad (1.9)$$

Since the studied polymer composite consists of several elements, the contribution of each to the radiation losses of the fast electron is determined by the expressions:

$$\left(-\frac{dE}{dx}\right)_{rad}^C = \rho_C \frac{Z_C^2}{A_C} G(E_k), \quad (1.10a)$$

$$\left(-\frac{dE}{dx}\right)_{rad}^{Si} = \rho_{Si} \frac{Z_{Si}^2}{A_{Si}} G(E_k), \quad (1.10b)$$

$$\left(-\frac{dE}{dx}\right)_{rad}^O = \rho_O \frac{Z_O^2}{A_O} G(E_k), \quad (1.10c)$$

$$\left(-\frac{dE}{dx}\right)_{rad}^H = \rho_H \frac{Z_H^2}{A_H} G(E_k), \quad (1.10d)$$

Then the total energy loss of the electron to radiation

$$\left(-\frac{dE}{dx}\right)_{rad} = \left(\rho_C \frac{Z_C^2}{A_C} + \rho_{Si} \frac{Z_{Si}^2}{A_{Si}} + \rho_O \frac{Z_O^2}{A_O} + \rho_H \frac{Z_H^2}{A_H} \right) G(E_k). \quad (1.11)$$

Fig. 1.2 presents the curves constructed on the basis of expressions (1.9) and (1.11), which show the total losses of fast electron radiation in the polymer composite (thicker curve) and the separate contribution of each chemical element of the composite to these losses. **Fig. 1.2** follows that the silicon component makes a greater contribution to radiation losses. Given the low density of the composite, the radiation energy losses are quite high, but they are small in comparison with the ionization losses at the considered electron energy values. In the general case, the energy losses of electrons in the studied polymer composite are determined by the sum of ionization and radiation losses (**Fig. 1.3**).

From **Fig. 1.3** it follows that at the considered values of electron energy, interesting from the point of view of electronic protection of the equipment in space, losses of energy of electron are generally defined by ionization of atoms.

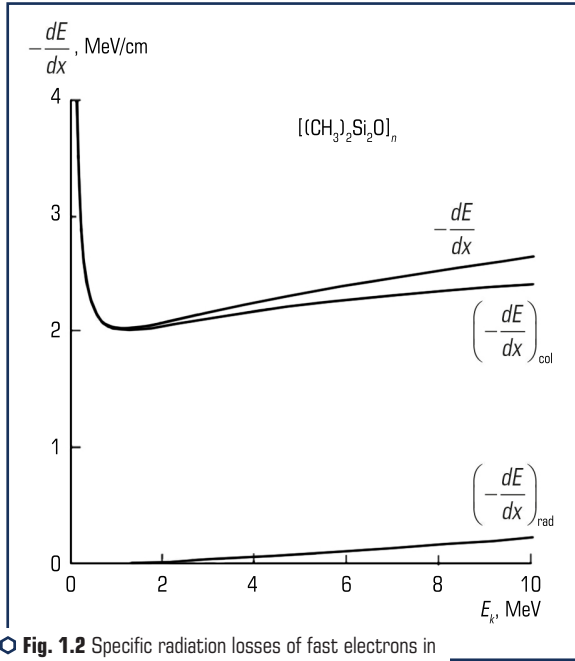


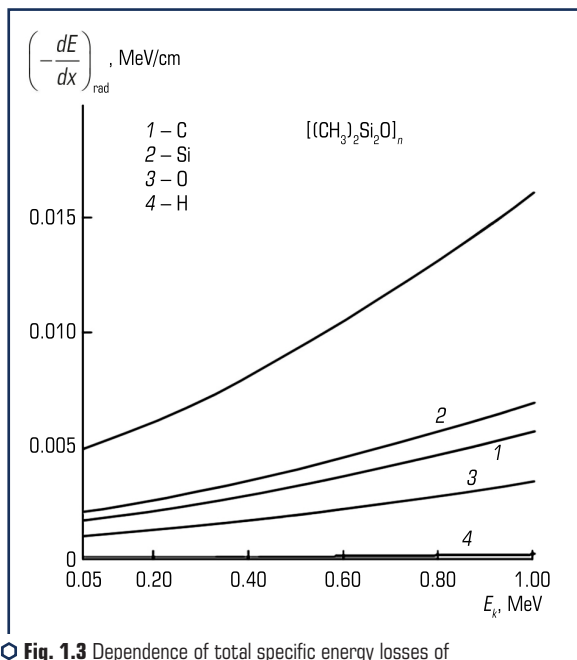
Fig. 1.2 Specific radiation losses of fast electrons in the polymer composite

Since the electron is "inhibited" by losses, let's find the average distance, which determines the average path length that the particle would travel in the process of deceleration in an unlimited and homogeneous medium, provided that it continuously loses energy along the entire path according to braking ability ($-dE/dx$). Real runs are random numbers and distributed around the average run. The average mileage is calculated by the formula:

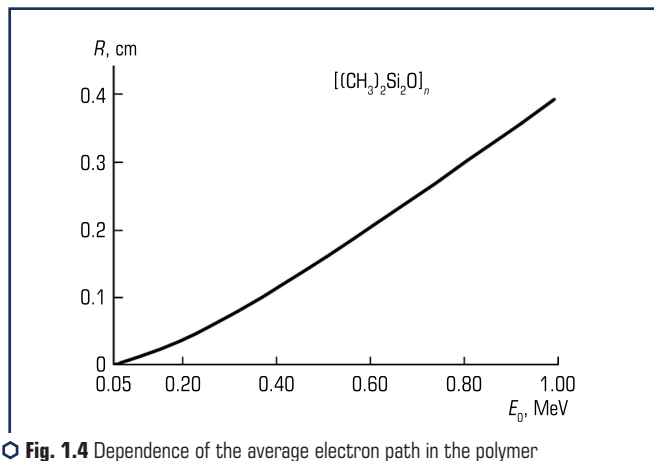
$$R(E_0) = \int_0^{E_0} \frac{dE_k}{\left(-\frac{dE}{dx}\right)}, \quad (1.12)$$

$$\text{where } \left(-\frac{dE}{dx}\right) = \left(-\frac{dE}{dx}\right)_{col} + \left(-\frac{dE}{dx}\right)_{rad}.$$

Fig. 1.4 and 1.5 show the dependences of the average electron path in the composite on its initial kinetic energy. The curves are constructed in different energy ranges.



○ **Fig. 1.3** Dependence of total specific energy losses of fast electrons in the studied polymer composite on the kinetic energy of electrons



○ **Fig. 1.4** Dependence of the average electron path in the polymer composite on its initial kinetic energy in the energy range from 0 to 1 MeV

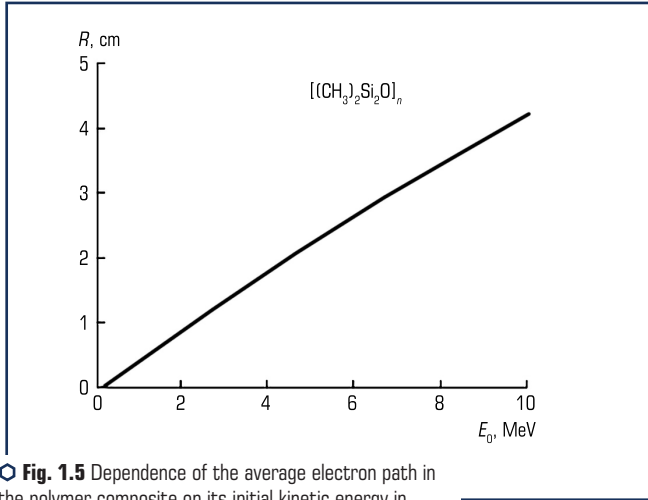


Fig. 1.5 Dependence of the average electron path in the polymer composite on its initial kinetic energy in the energy range from 0 to 10 MeV

Calculations show that the average electron path in the studied composite is quite small in a wide range of the initial energy of the electron, which indicates the prospects of its use to protect against the effects of electrons in outer space. Since fast electrons in outer space have a wide energy range and different orientations of the initial velocity, it is also necessary to investigate the electron transmission coefficients of this polymer composite.

Let's consider the transmittance of the number of particles and the energy of electrons incident on the material at an angle ϕ relative to the normal to its surface and pass a layer of matter with a thickness of x (**Fig. 1.6**):

$$T_N(x) = \frac{N(x)}{N_0}, \quad (1.13)$$

$$T_{E_x}(x) = \frac{E(x)}{N_0 E_0}. \quad (1.14)$$

Here N_0 and E_0 are the numbers of incident electrons and their kinetic energy. The Monte Carlo statistical method was used to simulate the process of electron transmission through the studied polymer composite.

Fig. 1.7–1.11 graphically present the results of modeling the dependence of the transmission coefficients on the number of particles and energy on the thickness of the composite for the angles and initial energies presented in the figures.

It is possible to make a conclusion about the high stability of the investigated composite in relation to a stream of fast electrons in the general case of their falling at various angles concerning normal to a target surface. A layer of such a composite, $x > 2$ cm thick, can completely shield the elements of electronic equipment from electron flows with energies up to 5 MeV.

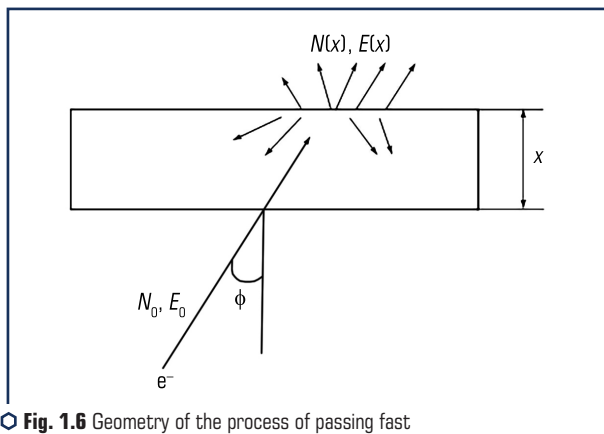


Fig. 1.6 Geometry of the process of passing fast electrons through a polymer composite

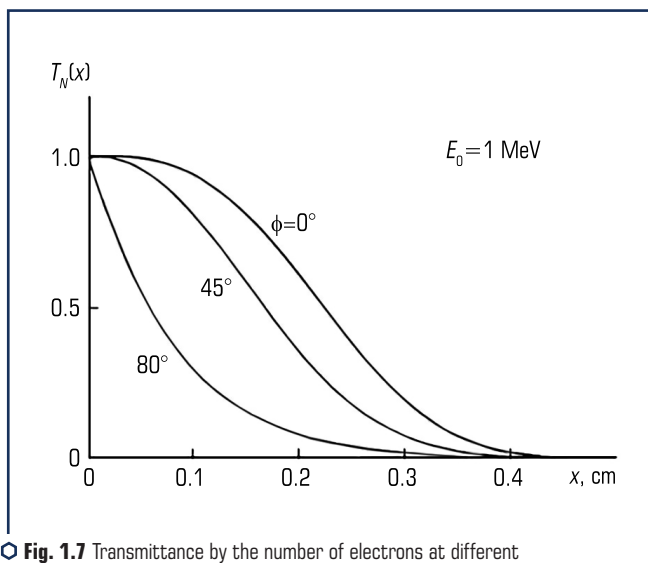


Fig. 1.7 Transmittance by the number of electrons at different angles of incidence

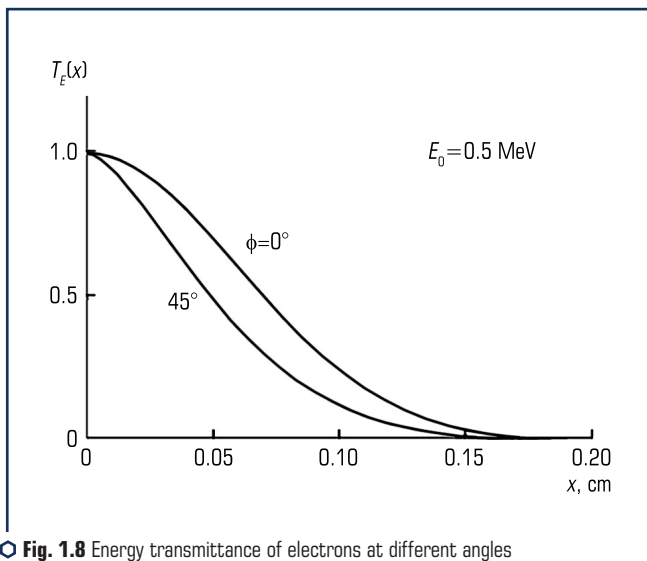


Fig. 1.8 Energy transmittance of electrons at different angles of incidence

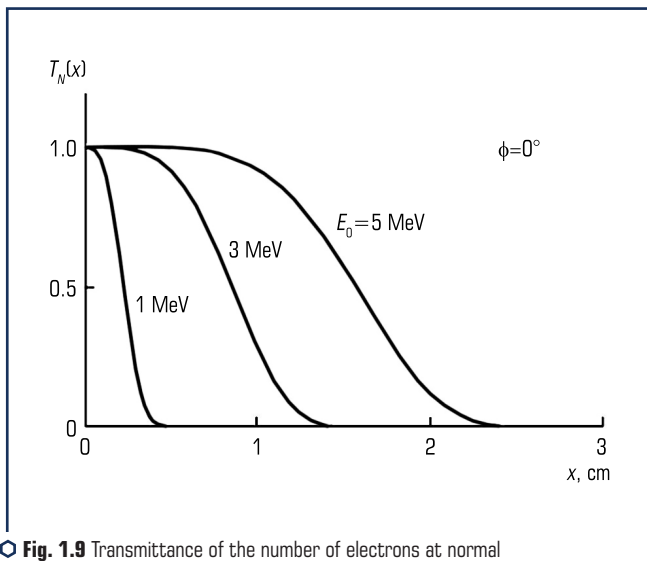


Fig. 1.9 Transmittance of the number of electrons at normal incidence on the composite for different initial electron energies

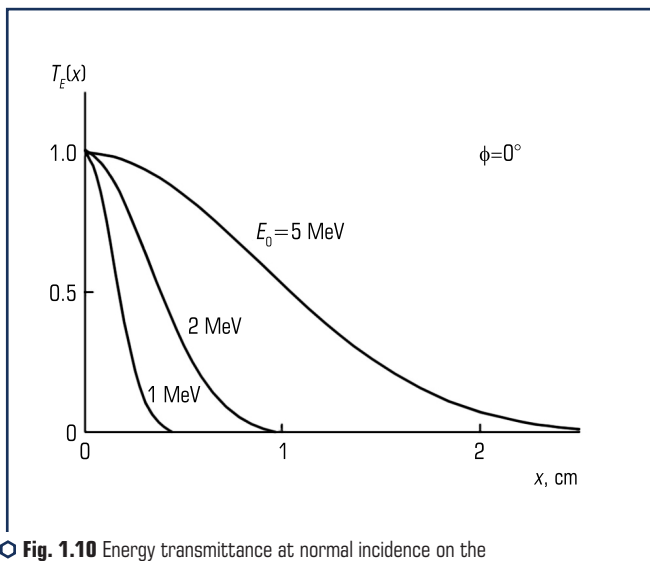


Fig. 1.10 Energy transmittance at normal incidence on the composite for different initial electron energies

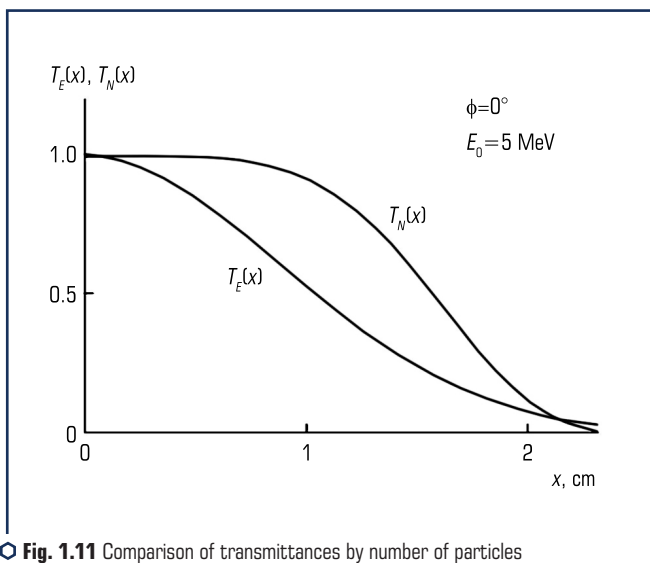


Fig. 1.11 Comparison of transmittances by number of particles and energy at normal incidence on the composite

1.2 THE METHOD OF INCREASING THE RADIATION RESISTANCE OF N-GE AND N-SI SINGLE CRYSTALS TO STREAMS OF HIGH-ENERGY ELECTRON IRRADIATION

Virtually all materials from which various structural units and working parts of nuclear and thermonuclear installations and spacecraft are made are exposed to radiation during their operation. Since, for example, the duration of nuclear reactors and designed thermonuclear devices must be at least 10 years (otherwise they will be economically unprofitable), at the same time must continuously "work" and structural materials [9, 10]. Reactor radiation, affecting the materials, changes their structure, and hence their strength, electrical and other properties. Radiation defects that are formed under such irradiations are mainly formed defects of the crystal structure (vacancies, between nodal atoms or their complexes with other impurities) [11, 12]. The energy transferred to a solid can lead to the rupture of interatomic bonds and the displacement of atoms with the formation of a primary radiation defect such as the Frenkel pair (vacancies and inter-nodal atom). Electromagnetic radiation (optical photons, γ -quanta, X-rays) directly disrupts the electronic system of the crystal, and only at the next stage are the various mechanisms of atomic displacement activated. The formation of radiation defects in the transfer of energy to electrons is possible in dielectrics and semiconductors. In metals, energy, quanta, or particles of radiation are usually spent on the excitation of atomic electrons and converted into heat without creating structural defects. The types and concentration of the formed stable radiation defects are determined both by the radiation conditions and by the properties of the solids themselves. In this case, the formation of stable point defects (isolated vacancies or internodal atoms, divacancies, complexes of Frenkel vapor components with impurity atoms) is most characteristic of light particles and photons of not very high energies.

The main criterion to which it is customary to pay attention when considering the behavior of materials in radiation fields is their ability to resist the action of radiation and retain their original properties. This characteristic of the material is called radiation resistance. Substances and materials differ significantly in their radiation resistance. This is due to differences in their physical and chemical properties: elemental composition, phase state, chemical and electronic state of molecules, structural defects. Radiation resistance significantly depends on the radiation environment, type of radiation, dose rate, ambient temperature, operating conditions. The first human-observed changes in materials under the influence of radiation were harmful, so the term "radiation damage to materials" appeared. Now, however, it is possible with the help of fast particles to purposefully change the structure of materials under certain conditions, thereby controlling their macroscopic properties. This opens wide opportunities for the application of radiation technologies in the production of, for example, crystals, and sometimes finished products from them with specially defined properties.

Semiconductor materials are widely used as various radiation detectors. Silicon or germanium diodes are used similarly to gas-filled ionization chambers to measure the spectral distribution of radiation quanta. The advantage of semiconductor detectors is that their ionization current is ten times greater than that of gases. Due to the higher density, the semiconductor absorbs much

more energy than gases. However, germanium and silicon detectors must be cooled to a temperature close to 200 °C and also use electronic pulse conversion circuits with low intrinsic noise. Currently, the task of ensuring the high performance of devices and equipment in the conditions of radiation exposure (electrons, protons, heavy charged particles, X-rays, and gamma radiation) is quite acute [13–17].

Radiation resistance of the equipment determines the term of its active use and trouble-free operation. This is especially true for electronic systems that are part of the onboard equipment of spacecraft [15]. Widespread use in the electronic equipment of the spacecraft of semiconductor devices and integrated circuits sensitive to the action of ionizing radiation of outer space, as well as increasing the service life of space objects requires ensuring the radiation resistance of micro-electronic elements for a given radiation environment.

Today, such methods of increasing the radiation resistance of silicon and germanium as nucle-
ar doping, pre-radiation heat treatment, doping with isovalent and electrically inactive impurities are used [18–20].

One of the promising areas of development of radiation-resistant equipment is the use of local protection methods, in particular the creation of special cases and coatings with integrated radiation shields [17]. These technologies allow the use of chips of commercial and industrial classes instead of radiation-resistant chips, which makes it possible to reduce the cost of onboard equipment and expand the range of components used. In this regard, it is practically and commercially advantageous to create protective screens, coatings, or shells of epoxy composite materials, which are more technological, lighter, and cheaper compared to metal cases. This requires detailed studies of the effect of radiation on the shielding capacity of such materials, especially when irradiated with high-energy particles.

In [21–23], the shielding ability of the epoxy composite coating layer from the effects of high-energy electron irradiation are investigated. This layer, 5 mm thick, which was an epoxy-diane resin brand ED-20 with PEPA hardener (12 parts by weight per 100 parts by weight of epoxy resin) without fillers and with fillers of iron and aluminum powders (30 parts by weight per 100 parts by weight of epoxy resin), was applied to the samples germanium and silicon. The investigated n-Ge and n-Si single crystals were grown by the Czochralski method and in the process of cultivation were doped with impurities of antimony and phosphorus, concentrations of $5 \cdot 10^{14} \text{ cm}^{-3}$ and $2.2 \cdot 10^{16} \text{ cm}^{-3}$, respectively.

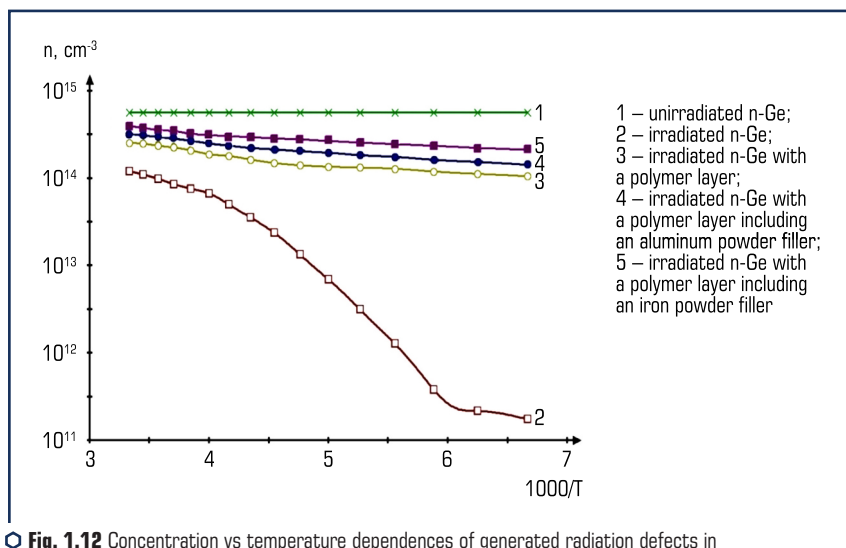
The method of obtaining samples of semiconductors and epoxy composites is described in detail in paragraph 1.2.

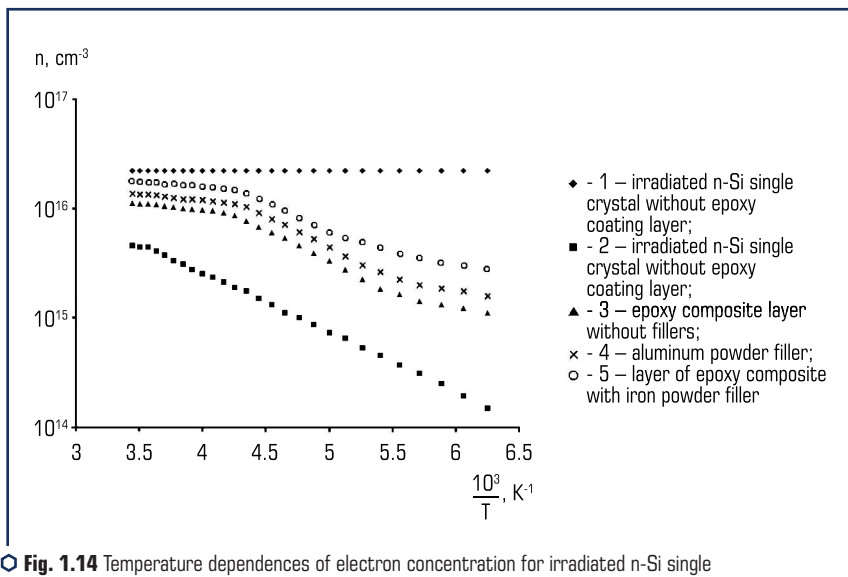
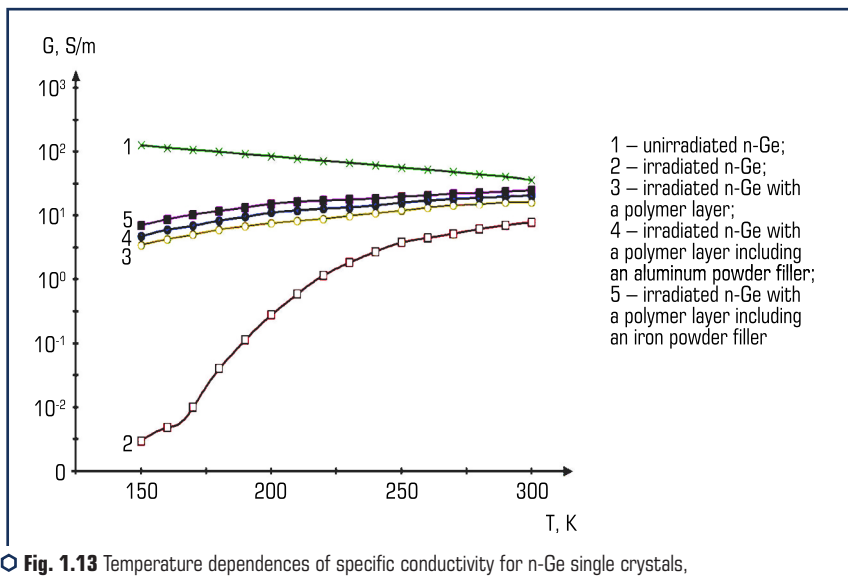
According to the experimental data of the authors [24], the dependence of the absorbed electron irradiation dose on the thickness of the polymer composite sample is extreme. The presence of a maximum for this dependence is associated with the development of the ionization process in the mass of the composite, which is caused by incident electrons and an increase in the ionization density of the medium due to the backscattering of secondary electrons at great depths. This leads to an increase in the absorbed radiation dose. It was also shown that with increasing energy of

the incident electron beam, this maximum expands and shifts in proportion to the thickness of the polymer composite. Therefore, as follows from these results, to reduce the transmittance of the electron irradiation flow, it is necessary to use either a very thick layer of polymer composite (for electron energy of 10 MeV it must be at least 50 mm) for the thickness at which the maximum is observed on the dependence of the absorbed dose. Therefore, in our research, let's choose the optimal coating layer of epoxy-diane resin with a thickness of 5 mm.

To study the shielding ability of such a layer of epoxy coating from electron irradiation, the temperature dependencies of electrical conductivity and Hall constant were measured for electron-irradiated electrons with energy 10 MeV and flow $\Omega=5 \cdot 10^{15}$ el./cm² n-Ge single crystals and irradiated electrons with energy 12 MeV and $\Omega=1 \cdot 10^{17}$ el./cm² n-Si single crystals coated with a layer of epoxy resin. In [25, 26], the temperature dependences of the electron concentration (Hall constant) for the same n-Si and n-Ge single crystals were obtained, irradiated with different streams of electrons.

As follows from these dependences, for electron irradiation flows $\Omega > 5 \cdot 10^{16}$ el./cm² and $\Omega > 5 \cdot 10^{16}$ el./cm² there is a significant decrease in the radiation resistance of the studied single crystals of silicon and germanium. With this in mind, it is chosen the above energies and electron irradiation flows of these single crystals. The temperature dependences of the concentration and specific electrical conductivity of the n-Si and n-Ge single crystals irradiated with electrons are presented in **Fig. 1.12–1.15**.





As follows from these dependencies, the electron concentration, specific conductivity, and, accordingly, radiation resistance increase for single crystals of germanium and silicon coated with a layer of epoxy-diane resin. The highest radiation resistance is achieved for n-Ge and n-Si samples coated with a layer of epoxy composite with an iron powder filler. According to the results of theoretical calculations, the average electron path in the polymer composite, in the first place, will be inversely proportional to the values of

$$B = \sum_{i=1}^n \rho_i \frac{Z_i}{A_i} \text{ and } C = \sum_{i=1}^n \rho_i \frac{Z_i^2}{A_i}.$$

Here ρ_i – the densities of the i -th chemical element, which is part of the macromolecule of the polymer composite, or filler, Z_i and A_i that respectively, their charge and mass numbers.

The values for $B_i = \rho_i \frac{Z_i}{A_i}$ and for $C_i = \rho_i \frac{Z_i^2}{A_i}$ the iron powder filler are larger than for the aluminum powder filler.

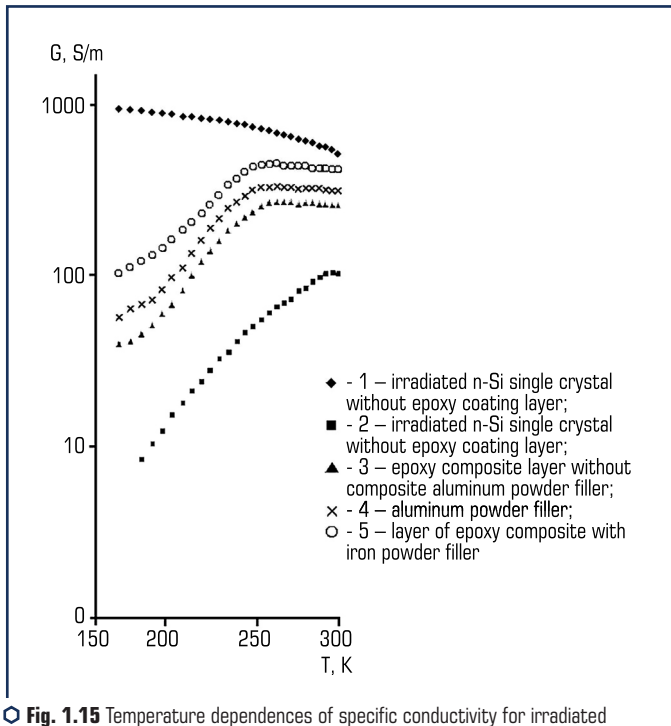


Fig. 1.15 Temperature dependences of specific conductivity for irradiated n-Si single crystals coated with a layer of epoxy resin

Therefore, the transmittance of the electron beam for a layer of epoxy composite with a filler of iron powder is less than for a layer of epoxy coating with a filler of aluminum powder. This explains the correspondingly higher radiation resistance of germanium samples coated with a layer of epoxy resin with iron powder filler than samples of germanium with a protective layer of epoxy resin filled with aluminum powder. A significant increase in the content of metallic filler in the epoxy polymer will reduce the densities of the chemical elements that are part of it, and in accordance with the weakening of the shielding capacity of the epoxy coating layer from radiation. Therefore, in our studies, let's choose the content of fillers of iron and aluminum powders, not exceeding 30 wt. including when this effect will be little noticeable. The increase in electron concentration and specific conductivity for irradiated n-Ge and n-Si single crystals coated with an epoxy coating layer is associated with a decrease in the concentration of radiation defects with deep acceptor levels in such single crystals due to attenuation of electron beam energy during epoxy composition. In [25] based on the measurements of infrared Fourier spectroscopy, Hall effect, and tenso-Hall effect, the nature and concentration of the main types of radiation defects for n-Si single crystals were determined. It was found that the main radiation defects formed by electron irradiation are A-centers (VO_2 complexes), complexes containing internodal carbon (C_2O_2 complexes), and VO_2P complexes (A-center modified with phosphorus). Irradiation of n-Ge samples with electron flows with an energy of 10 MeV leads to the formation of both point defects belonging to the VOI_2 complexes (A-center – two internodal germanium atoms) and order regions [27, 28]. The decrease in the concentration and specific conductivity of these samples with decreasing temperature is explained by the deionization of the deep acceptor level of $E_c-0.27$ eV belonging to the A-center. To quantify the level of defects in the studied single crystals of silicon and germanium, calculations of the concentration of formed radiation defects were performed. To do this, as shown in [25, 26], a system of equations of electroneutrality was solved. The results of such calculations are presented in **Tables 1.2 and 1.3**.

● **Table 1.2** Concentration of radiation defects in irradiated silicon single crystals coated with an epoxy composite layer single crystals coated with an epoxy composite layer

Sample type	Irradiated single crystal n-Si (without coating with a layer of epoxy composite)	Irradiated n-Si single crystal covered with a layer of epoxy composite	Irradiated n-Si single crystal coated with a layer of epoxy composite with aluminum powder filler	Irradiated n-Si single crystal coated with a layer of epoxy composite with iron powder filler
Concentration of complexes $\text{VO}_2\text{P}_{\text{N}_1}$, cm^{-3}	$1 \cdot 10^{16}$	$8.5 \cdot 10^{15}$	$6.6 \cdot 10^{15}$	$4.2 \cdot 10^{15}$
Concentration of complexes VO_2N_2 , cm^{-3}	$2.5 \cdot 10^{14}$	$1.7 \cdot 10^{14}$	$1.3 \cdot 10^{14}$	$7.1 \cdot 10^{13}$
Concentration of complexes $\text{C}_2\text{O}_2\text{N}_3$, cm^{-3}	$7.4 \cdot 10^{15}$	$2.3 \cdot 10^{15}$	$1.6 \cdot 10^{15}$	$2.9 \cdot 10^{13}$

• **Table 1.3** Concentration of radiation defects in irradiated germanium samples coated with epoxy composite layer

Sample type	Irradiated n-Ge single crystal (without epoxy composite layer coating)	Irradiated n-Ge single crystal covered with a layer of epoxy composite	Irradiated n-Ge single crystal covered with a layer of epoxy composite	Irradiated n-Ge single crystal coated with a layer of epoxy composite with iron powder filler
Concentration of A-centers N , cm^{-3}	$2.8 \cdot 10^{14}$	$2.3 \cdot 10^{14}$	$1.9 \cdot 10^{14}$	$1.6 \cdot 10^{14}$

As follows from **Tables 1.2 and 1.3**, the presence of a protective layer of epoxy composite leads to a decrease in the concentration of radiation defects in n-Si and n-Ge single crystals, especially when this protective layer contains an iron powder filler. In this case, for the irradiated n-Si, the concentration of the formed radiation defects corresponding to the VO_2P and VO_2 complexes decreases several times, and the C_2O_2 complexes decrease by more than two orders of magnitude.

A similar situation is observed for irradiated n-Ge single crystals. Therefore, the presence of a protective layer of epoxy composite significantly increases the radiation resistance of n-Si and n-Ge single crystals. The introduction into the polymer matrix of fillers of aluminum and iron powders leads to an increase in the shielding ability of such a layer from radiation. The obtained layer of epoxy-diane resin brand ED-20 with PEPA hardener (12 parts by weight) (without fillers) and with fillers of iron and aluminum powders (30 parts by weight) can be a promising material for creating cheap protective coatings for semiconductor electronics, which made on the basis of silicon and germanium, from the aggressive action of high-energy electron irradiation.

1.3 MAGNETIC SENSITIVITY OF ELECTRON-IRRADIATED N-GE AND N-SI SINGLE CRYSTALS COATED WITH AN EPOXY COMPOSITE LAYER

Interest in magnetic field sensors has not waned for several decades, due to the development of a large number of electronic devices that work on the basis of measurements of magnetic field parameters [29]. These include non-contact DC meters and switches, pipeline diagnostics and information input systems, motion meters in automotive and aerospace products, tomographs in medicine, Hall sensors for nuclear, thermonuclear energy, and research [30, 31]. Such a wide scope of operation of magnetic field sensors puts forward a number of requirements for them: increase of radiation resistance and range of operating temperatures; reduction of power consumption; size reduction; placement on one crystal of all elements that simultaneously measure different components of the magnetic field. In particular, in charged particle accelerators, nuclear and thermonuclear reactors, the magnetic field is measured under radiation conditions, so the efficiency and reliability of magnetic field sensors depend on the stability of their characteristics. This puts forward the requirements of increased radiation resistance to semiconductor materials,

on the basis of which the sensitive elements of Hall sensors are made [32]. Materials such as Si are used to make semiconductor Hall sensors; Ge; HgTe; HgSe; GaAs; InSb; InAs and others. In this respect, monocrystalline silicon and germanium occupy advanced positions due to their unique properties, commercial availability, and well-developed cultivation technology [33]. In the practical use of Hall sensors, there are two types of tasks. In one case, it is necessary to obtain the maximum, at a given scattering power, the EMF Hall, and the input resistance of the circuit can be arbitrarily large. In the second case, the goal is to get the maximum power in the Hall circuit. To implement the optimal in its parameters Hall sensors, working on the first principle, it is necessary to make them from a material having a low concentration of charge carriers of one sign, i.e. a large value of the Hall constant. In the second case, to match the sensor with the device, the material must meet two conditions: the resistance of the sample should not be too small and the mobility of the charge carriers should be high enough. When operating Hall sensors in conditions of radiation exposure, along with high radiation resistance, it is necessary to ensure their protection from the aggressive effects of the environment and various physical fields. One way to solve this complex problem is to develop simple, lightweight, relatively inexpensive, and technological protective coatings for the magnetically sensitive element of the Hall sensor. In this sense, epoxy composites are promising materials, given the above characteristics.

Therefore, it is interesting from a practical point of view to develop protective coatings based on epoxy-composite materials for silicon single crystals, which can be used to design a magnetically sensitive element of Hall sensors operating in conditions of high radiation.

In [23, 34], the magnetic sensitivity of electron-irradiated n-Ge and n-Si single crystals coated with a layer of epoxy resin (without fillers and with fillers of aluminum and iron powders) are researched. The conditions of electron irradiation, characteristics of the studied single crystals of silicon and germanium, epoxy coating layer, and methods of preparation of samples for research, experimental measurements were the same as in studies of radiation resistance of these single crystals. In [34], the effect of electron irradiation with an energy of 10 MeV and a flow $\Omega = 5 \cdot 10^{15}$ el./cm² on the magnetic sensitivity of n-Ge single crystals coated with an epoxy composite layer was investigated. As a result of measurements of the Hall effect, the dependences of the Hall voltage U_H on the induction of the magnetic field B at different temperatures were obtained.

As follows from these figures, the dependences $U_H = f(B)$ are linear for germanium single crystals coated with a layer of epoxy resin without filler and with a filler of aluminum powder in the entire range of the studied magnetic fields. These dependencies indicate a secondary role of the magnetoresistance effect, which can be manifested for germanium single crystals with oxygen-containing complexes at higher values of magnetic fields [35]. For germanium samples coated with a layer of epoxy composite with an iron powder filler, there is a slight deviation from the linearity of the dependence $U_H = f(B)$ at magnetic fields up to 0.3 T (**Fig. 1.16–1.18, curves 4**).

This can be explained by the fact that when such samples are placed in a magnetic field, the iron powder is magnetized, the magnetic field of which additionally affects the germanium sample

and thus changes the EMF of Hall. Confirmation of the existence of an additional magnetic field is the presence of residual magnetization, which creates an EMF Hall, after the "exclusion" of the external magnetic field.

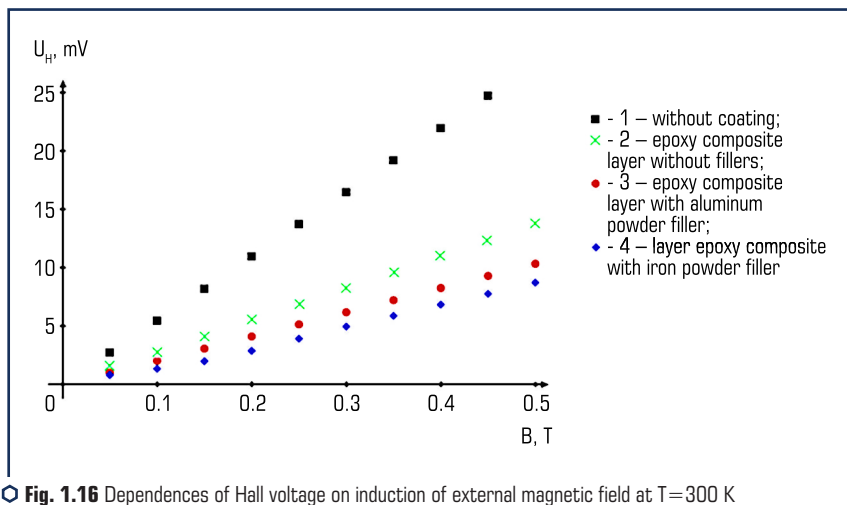


Fig. 1.16 Dependences of Hall voltage on induction of external magnetic field at $T=300$ K for irradiated n-Ge single crystals with different type of outer coating layer

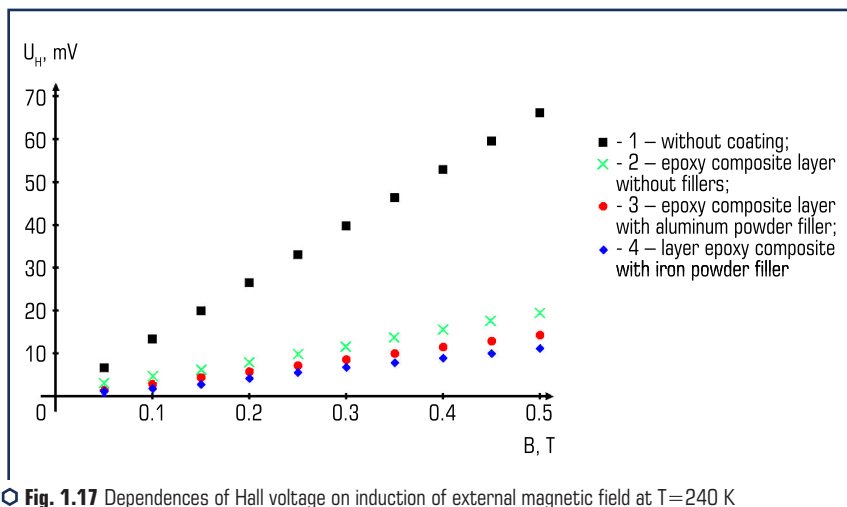


Fig. 1.17 Dependences of Hall voltage on induction of external magnetic field at $T=240$ K for irradiated n-Ge single crystals with different type of outer coating layer

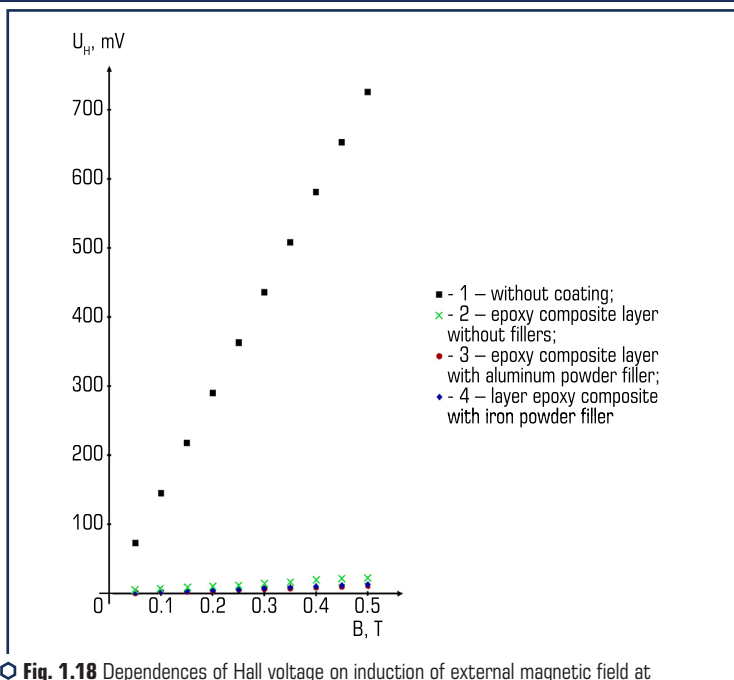


Fig. 1.18 Dependences of Hall voltage on induction of external magnetic field at $T = 190$ K for irradiated n-Ge single crystals with different type of outer coating layer

The dependences of the Hall EMF on time in the absence of an external magnetic field for different temperatures are shown in Fig. 1.19.

As follows from Fig. 1.19, the residual magnetization of iron powder, which is a filler for epoxy resin, creates a Hall EMF of 2.123 mV, 1.967 mV and 1.552 mV at temperatures of 190 K, 240 K, and 300 K, respectively. The EMF of Hall decreases most rapidly (more than 10 times in 2 hours) at $T = 300$ K (Fig. 1.4, curve 3). This is due to the fact that the increase in temperature leads to a decrease in the degree of directional orientation of the magnetic fields of individual domains of iron powder [36]. Similar dependences of the Hall EMF on the induction of an external magnetic field at temperatures $T = 290$ K and $T = 200$ K (Fig. 1.20 and 1.21) were obtained for n-Si single crystals in [23].

These dependencies are linear with the exception of silicon single crystals coated with a layer of epoxy composite with an iron powder filler, for which, as for n-Ge single crystals, there is a slight deviation from the linearity of the dependence $U_H = f(B)$ at magnetic fields up to 0.3 T (Fig. 1.21, curve 5), which is explained by the presence of additional magnetization of iron powder, which changes the EMF of Hall.

The dependencies of the EMF Hall on time in the absence of an external magnetic field for n-Si samples coated with a layer of epoxy resin with iron powder filler are shown in Fig. 1.22.

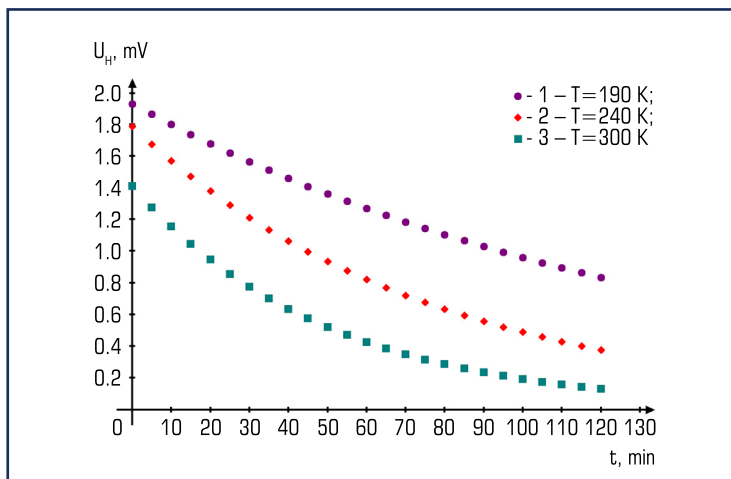


Fig. 1.19 Dependence of $U_x(t)$ when field magnetized $B=0.5$ T for irradiated n-Ge single crystals coated with a layer of epoxy composite with an iron powder filler

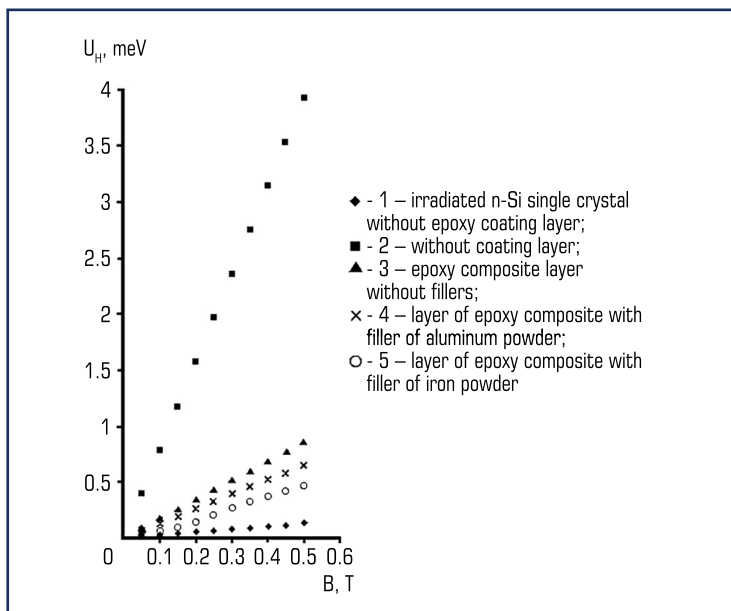


Fig. 1.20 Dependences of Hall EMF on the induction of an external magnetic field at $T=290$ K for irradiated n-Si single crystals coated with a layer of epoxy resin

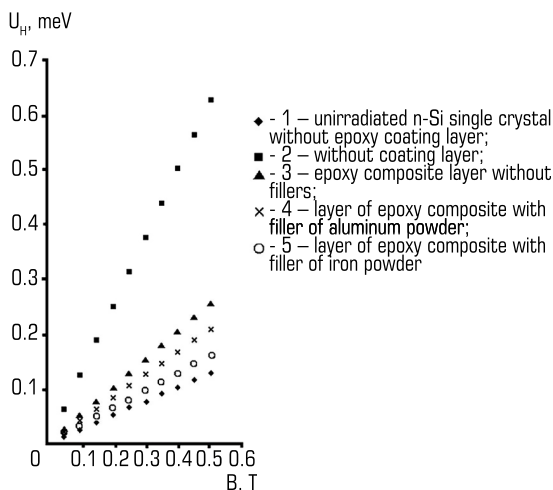


Fig. 1.21 Dependences of Hall EMF on the induction of an external magnetic field at $T=200$ K for irradiated n-Si single crystals coated with a layer of epoxy resin

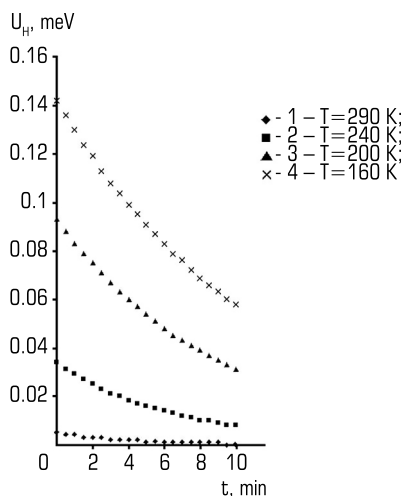


Fig. 1.22 Dependence of Hall EMF during field magnetization $B=0.5$ T on time for irradiated n-Si single crystals coated with a layer of epoxy resin with an iron powder filler

As for germanium single crystals, for silicon single crystals the residual magnetization of iron powder increases with decreasing temperature. At a temperature $T=290$ K, the additionally induced Hall EMF is only $5 \mu\text{V}$ (**Fig. 1.22, curve 1**), so it does not affect the linearity of the dependence $U_H=f(B)$ (**Fig. 1.20, curve 5**). To calculate the magnetic sensitivity of the studied n-Ge and n-Si single crystals, the analytical dependences of the EMF Hall on the induction of an external magnetic field were obtained using the least-squares method. Approximation polynomials for the calculation of such dependencies are presented in **Tables 1.4–1.8**.

● **Table 1.4** Approximation polynomials for calculation of Hall EMF and magnetic sensitivity at $T=300$ K for irradiated germanium samples coated with a protective layer of epoxy resin

Sample type	Dependence of EMF Hall U_H (meV) on the induction of an external magnetic field B (T)	Dependence of magnetic sensitivity $\beta=\delta U_H/\delta B$ (meV/T) on the induction of an external magnetic field B (T)
Irradiated n-Ge single crystal without a protective layer of epoxy coating	$U_H=55V$	55
Irradiated n-Ge single crystal covered with a layer of epoxy resin	$U_H=27.51V$	27.51
Irradiated n-Ge single crystal coated with an epoxy layer with aluminum powder filler	$U_H=20.75V$	20.75
Irradiated n-Ge single crystal coated with a layer of epoxy resin with an iron powder filler	$U_H = \begin{cases} 28.89V^2 + 6.659V + 0.43, & V < 0.3; \\ 18.92V, & V \geq 0.3 \end{cases}$	$\beta = \begin{cases} 57.78V + 6.659, & V < 0.3; \\ 18.92, & V \geq 0.3 \end{cases}$

● **Table 1.5** Approximation polynomials for the calculation of Hall EMF and magnetic sensitivity at $T=240$ K for irradiated germanium samples coated with a protective layer of epoxy resin

Sample type	Dependence of EMF Hall U_H (meV) on the induction of an external magnetic field B (T)	Dependence of magnetic sensitivity $\beta=\delta U_H/\delta B$ (meV/T) on the induction of an external magnetic field B (T)
1	2	3
Irradiated n-Ge single crystal without a protective layer of epoxy coating	$U_H=132V$	132
Irradiated n-Ge single crystal covered with an epoxy layer	$U_H=38.9V$	38.9
Irradiated n-Ge single crystal coated with a layer of epoxy resin with aluminum powder filler	$U_H=28.44V$	28.44

• Continuation of Table 1.5

1	2	3
Irradiated n-Ge single crystal coated with a layer of epoxy resin with iron powder filler	$U_H = \begin{cases} 30,12V^2 + 12,6V + 0,276, \\ V < 0,3; \\ 22,08V, \\ V \geq 0,3 \end{cases}$	$\beta = \begin{cases} 60,24V + 12,6, \\ V < 0,3; \\ 22,08, \\ V \geq 0,3 \end{cases}$

• Table 1.6 Approximation polynomials for the calculation of Hall EMF and magnetic sensitivity at T=190 K for irradiated germanium samples coated with a protective layer of epoxy resin

Sample type	Dependence of EMF Hall U_H (meV) on the induction of an external magnetic field B (T)	Dependence of magnetic sensitivity $\beta = \delta U_H / \delta B$ (meV/T) on the induction of an external magnetic field B (T)
Irradiated n-Ge single crystal without a protective layer of epoxy coating	$U_H = 1452V$	1452
Irradiated n-Ge single crystal covered with an epoxy layer	$U_H = 52.7V$	52.7
Irradiated n-Ge single crystal coated with a layer of epoxy resin with aluminum powder filler	$U_H = 36.5V$	36.5
Irradiated n-Ge single crystal coated with a layer of epoxy resin with iron powder filler	$U_H = \begin{cases} 32,85V^2 + 13,55V + 0,54, \\ V < 0,3; \\ 26,74V, \\ V \geq 0,3 \end{cases}$	$\beta = \begin{cases} 65,7V + 13,55, \\ V < 0,3; \\ 26,74, \\ V \geq 0,3 \end{cases}$

• Table 1.7 Approximation polynomials for the calculation of Hall EMF and magnetic sensitivity at T=290 K for unirradiated and irradiated silicon single crystals coated with a protective layer of epoxy resin

Sample type	Dependence of EMF Hall U_H (meV) on the induction of an external magnetic field B (T)	Dependence of magnetic sensitivity $\beta = \delta U_H / \delta B$ (meV/T) on the induction of an external magnetic field B (T)
1	2	3
Irradiated n-Si single crystal without a protective layer of epoxy coating	$U_H = 1.257V$	1.257
Irradiated n-Si single crystal coated with a layer of epoxy resin	$U_H = 0.509V$	0.509
Irradiated n-Si single crystal coated with an epoxy layer with aluminum powder filler	$U_H = 0.42V$	0.42

● Continuation of Table 1.7

1	2	3
Irradiated n-Si single crystal coated with a layer of epoxy resin and filled with iron powder	$U_H = 0.32V$	0.32
Non-irradiated n-Si single crystal without a protective layer of epoxy coating	$U_H = 0.257V$	0.257

As follows from the tables, the magnetic sensitivity of single crystals of silicon and germanium increases with decreasing temperature, as the concentration of electrons in the conduction band of silicon decreases and the Hall constant increases, which determines the value of magnetic sensitivity. For n-Ge and n-Si single crystals coated with a layer of epoxy resin without fillers and with aluminum powder filler, the magnetic sensitivity does not depend on the induction of an external magnetic field, and for the case of such single crystals coated with a layer of epoxy resin with iron powder filler, increases linearly with increasing magnetic field to 0.3 T. The least-squares approximation polynomials obtained for the calculation of Hall EMF and magnetic sensitivity can be used in the construction of radiation-resistant magnetically sensitive elements for Hall sensors based on germanium and silicon single crystals coated with a layer of epoxy resin.

● **Table 1.8** Approximation polynomials for the calculation of Hall EMF and magnetic sensitivity at $T = 200$ K for irradiated silicon single crystals coated with a protective layer of epoxy resin

Sample type	Dependence of EMF Hall U_H (mV) on the induction of an external magnetic field B (T)	Dependence of magnetic sensitivity $\beta = \delta U_H / \delta B$ (mV/T) on the induction of an external magnetic field B (T)
Irradiated n-Si single crystal without a protective layer of epoxy coating	$U_H = 7.85V$	7.85
Irradiated n-Si single crystal coated with a layer of epoxy resin	$U_H = 1.717V$	1.717
Irradiated n-Si single crystal coated with an epoxy layer with aluminum powder filler	$U_H = 1.303V$	1.303
Irradiated n-Si single crystal coated with a layer of epoxy resin and filled with iron powder	$U_H = \begin{cases} 2,757V^2 - 0,054V + 0,041, & V < 0,3; \\ 0,928V, & V \geq 0,3 \end{cases}$	$\beta = \begin{cases} 5,514V - 0,054, & V < 0,3; \\ 0,928, & V \geq 0,3 \end{cases}$
Non-irradiated n-Si single crystal without a protective layer of epoxy coating	$U_H = 0.257V$	0.257

The epoxy coating layer will also provide additional protection of the magnetosensitive element from moisture, vibration, rapidly changing temperature fields, and electromagnetic radiation, which will allow the use of such Hall sensors in harsher operating conditions.

The presence of residual magnetization of the iron powder filler and the corresponding induced additional Hall EMF can be of practical importance in the development of energy storage systems based on irradiated n-Ge and n-Si single crystals coated with a layer of epoxy resin with iron powder filler.

CONCLUSIONS

1. It is established that the most radiation-resistant to high-energy electron irradiation are n-Ge and n-Si single crystals covered with a layer of epoxy coating with an iron powder filler containing 30 parts by weight on 100 parts by weight including the epoxy resin. This is due to the fact that for iron filler there is an optimal ratio between its density, mass, and charge numbers, due to which the average electron path in the polymer composite will be the lowest compared to the layer of the epoxy composite without fillers and aluminum powder filler.

2. The dependences of the EMF Hall on the induction of an external magnetic field at different temperatures for electron-irradiated n-Ge single crystals (energy 10 MeV and flow $\Omega = 5 \cdot 10^{15}$ el./cm²) and n-Si (energy 12 MeV and flow $\Omega = 1 \cdot 10^{17}$ el./cm²) coated with a layer of epoxy-diane resin brand ED-20 with the content of PEPA hardener 12 parts by weight on 100 parts by weight including epoxy resin, both without fillers and with fillers of iron and aluminum powders with mass fractions of 30 %.

From the analysis of these dependencies it follows that they are linear for single crystals of germanium and silicon, coated with a layer of epoxy resin without fillers and with fillers of aluminum powder in the whole range of the studied magnetic fields.

For n-Ge and n-Si samples coated with a layer of epoxy resin with iron powder filler, there is a slight deviation from the linearity of such dependences at magnetic fields up to 0.3 T, which is explained by additional magnetization of iron powder.

The presence of residual magnetization can be used to develop on the basis of data from single crystals of energy storage systems.

3. It was established that the residual magnetization of the iron powder filler in the epoxy coating layer leads to the emergence of Hall EMF in n-Ge and n-Si single crystals. This will be able to find its practical use in the development of energy storage systems based on such single crystals.

4. Experimental researches of radiation resistance of n-Ge and n-Si single crystals can be used in the development and modeling based on epoxy resin with fillers of aluminum and iron powders of relatively cheap, light, and technological protective coatings of sensitive elements sensors made on the basis of silicon and germanium, or cases of semiconductor devices for nuclear and thermonuclear energy, aerospace industry, scientific research.

CONFLICT OF INTEREST

The authors declare that they have no conflict of interest in relation to this research, whether financial, personal, authorship or otherwise, that could affect the research and its results presented in this paper.

REFERENCES

1. Klym, H., Ingram, A., Shpotyuk, O., Filipecki, J., Hadzaman, I. (2007). Extended positron-trapping defects in insulating MgAl_2O_4 spinel-type ceramics. *Physica status solidi (c)*, 4 (3), 715–718. doi: <https://doi.org/10.1002/pssc.200673735>
2. Klym, H., Karbovnyk, I., Luchechko, A., Kostiv, Y., Pankratova, V., Popov, A. I. (2021). Evolution of Free Volumes in Polycrystalline BaGa_2O_4 Ceramics Doped with Eu^{3+} Ions. *Crystals*, 11 (12), 1515. doi: <https://doi.org/10.3390/cryst11121515>
3. Karbovnyk, I., Borshchysyn, I., Vakhula, Ya., Lutsyuk, I., Klym, H., Bolesta, I. (2016). Impedance characterization of Cr^{3+} , Y^{3+} and Zr^{4+} activated forsterite nanoceramics synthesized by sol-gel method. *Ceramics International*, 42 (7), 8501–8504. doi: <https://doi.org/10.1016/j.ceramint.2016.02.075>
4. Luniov, S. V., Burban, O. V., Nazarchuk, P. F. (2015). Electron scattering in the Δ_1 model of the conduction band of germanium single crystals. *Semiconductors*, 49 (5), 574–578. doi: <https://doi.org/10.1134/s1063782615050140>
5. Luniov, S. V., Nazarchuk, P. F., Burban, O. V. (2013). Parameters of the high-energy Δ_1 -minimum of the conduction band in n-Ge. *Journal of Physical Studies*, 17 (3). doi: <https://doi.org/10.30970/jps.17.3702>
6. Fedosov, A. V., Luniov, S. V., Fedosov, S. A. (2011). Influence of uniaxial deformation on the filling of the level associated with A-center in n-Si crystals. *Ukrainian Journal of Physics*, 56 (1), 69–73. doi: <https://doi.org/10.15407/ujpe56.1.69>
7. Pavlenko, V. I., Edamenko, O. D., Cherkashina, N. I., Noskov, A. V. (2014). Total energy losses of relativistic electrons passing through a polymer composite. *Journal of Surface Investigation. X-Ray, Synchrotron and Neutron Techniques*, 8 (2), 398–403. doi: <https://doi.org/10.1134/s1027451014020402>
8. Storm, L., Israel, H. I. (1970). Photon cross sections from 1 keV to 100 MeV for elements $Z=1$ to $Z=100$. *Atomic Data and Nuclear Data Tables*, 7 (6), 565–681. doi: [https://doi.org/10.1016/s0092-640x\(70\)80017-1](https://doi.org/10.1016/s0092-640x(70)80017-1)
9. Smirnov, L. S. (Ed.) (1980). *Voprosy radiatsionnoi tekhnologii poluprovodnikov*. Novosibirsk: Nauka.
10. Koshkin, V. M., Volovichev, I. N., Gurevich, Yu. G., Gal'chinet'skiy, L. P., Rarenko, I. M. (2006). *Materialy i ustroystva s gigantskim radiatsionnym resursom. Materialy stcintilliatcionnoi tekhniki*, 60.

11. Uglov, V. V. (2007). Radiatsionnye efekty v tverdykh telakh. Minsk: BSU, 167.
12. Brudny, V. N. (2005). Radiatsionnye efekty v poluprovodnikakh. Vestnik Tomskogo gosudarstvennogo universiteta, 285, 95–102.
13. Bagatin, M., Gerardin, S. (2016). Ionizing radiation effects in electronics: from memories to imagers. CRC press, 412. doi: <https://doi.org/10.1201/b19223>
14. Schrimpf, R. D. (2007). Radiation Space Environment. Radiation Effects in Microelectronics. Springer, 11–29.
15. Novikov, L. S. (2010). Radiatsionnye vozdeistviia na materialy kosmicheskikh apparatov. Moscow: Universitetskaya kniga, 192.
16. Vasilenkov, N., Maksimov, A., Grabchikov, S., Lastovskiy, S. (2015). Special-Propose Radiation Protective Packages for Microelectronics Devices. Electronics: Science, Technology, Business, 4, 50–56. Available at: <https://www.electronics.ru/journal/article/4657>
17. Zeynali, O., Masti, D., Gandomkar, S. (2012). Shielding protection of electronic circuits against radiation effects of space high energy particles. Advances in Applied Science Research, 3 (1), 446–451.
18. Barabash, L. I., Vishnevsky, I. M., Groza, A. A., Karpenko, A. Ya., Litovchenko, P. G., Starchik, M. I. (2007). Modern methods of the increase of the semiconductor materials radiation hardness. Problems of Atomic Science and Technology, 2, 182–189.
19. Dezillie, B., Li, Z., Eremin, V., Chen, W., Zhao, L. J. (2000). The effect of oxygen impurities on radiation hardness of FZ silicon detectors for HEP after neutron, proton and gamma irradiation. IEEE Transactions on Nuclear Science, 47 (6), 1892–1897. doi: <https://doi.org/10.1109/23.914465>
20. Litovchenko, P. G., Barabash, L. Y., Berdnyichenko, S. V., Varnyina, V. Y., Groza, A. A., Dolgolenko, O. P. (2009). Influence of impurities on the radiation stability of the silicon. Voprosy atomnoi nauki i tekhniki, 2 (93), 39–42.
21. Udovyt'ska, Yu. A., Maslyuk, V. T. (2020). Development of epoxy composite protective coatings for increasing the radiation stability of n-Ge single crystals. Functional Materials, 27 (1), 24–28. doi: <https://doi.org/10.15407/fm27.01.24>
22. Udovyt'ska, Yu. A., Luniov, S. V., Kashytskyi, V. P., Khvyshchun, M. V., Tsy, A. I., Maslyuk, V. T. (2020). Vykorystannia epoksykompozytiv dlia pidvyshchennia radiatsiinoi stiiokosti monokrystaliv n-Ge. Relaksatsiino, nelineino, akustooptychni protsesy i materialy. Luts'k, 101–103.
23. Udovyt'ska, Yu. A., Luniov, S. V., Kashytskyi, V. P., Maslyuk, V. T. (2021). Effect of Epoxy Composite Coatings on Radiation Stability and Magnetic Sensitivity of n-Si Single Crystals. Surface Engineering and Applied Electrochemistry, 57 (2), 222–227. doi: <https://doi.org/10.3103/s1068375521020125>
24. Pavlenko, V. I., Yastrebinskiy, R. N., Edamenko, O. D., Tarasov, D. G. (2010). Affecting of high-power bunches of rapid electrons polymeric radiation-protective kompozity. Problems of atomic science and technology, 1 (65), 129–134. Available at: https://vant.kipt.kharkov.ua/ARTICLE/VANT_2010_1/article_2010_1_129.pdf

25. Luniov, S., Zimych, A., Khvyshchun, M., Yevsiuk, M., Maslyuk, V. (2018). Specific features of defect formation in the nSi <P> single crystals at electron irradiation. *Eastern-European Journal of Enterprise Technologies*, 6 (12 (96)), 35–42. doi: <https://doi.org/10.15587/1729-4061.2018.150959>
26. Luniov, S. V., Zimych, A. I., Nazarchuk, P. F., Maslyuk, V. T., Megela, I. G. (2016). Radiation defects parameters determination in n-Ge single crystals irradiated by high-energy electrons. *Nuclear Physics and Atomic Energy*, 17 (1), 47–52. doi: <https://doi.org/10.15407/jnpae2016.01.047>
27. Luniov, S. V., Zimych, A. I., Nazarchuk, P. F., Maslyuk, V. T., Megela, I. G. (2015). The impact of radiation defects on the mechanisms of electron scattering in single crystals n-Ge. *Journal of Physical Studies*, 19 (4). doi: <https://doi.org/10.30970/jps.19.4704>
28. Luniov, S. V., Khvyshchun, M. V., Tsy, A. I., Maslyuk, V. T. (2021). Influence of Electron Irradiation and Annealing on the IR Absorption of Germanium Single Crystals. 2021 IEEE 12th International Conference on Electronics and Information Technologies (ELIT), 18–22. doi: <https://doi.org/10.1109/ELIT53502.2021.9501152>
29. Tumanski, S. (2013). Modern magnetic field sensors: a review. *Przeglad elektrotechniczny*, 10, 1–12.
30. Ripka, P. (2010). Electric current sensors: a review. *Measurement Science and Technology*, 21 (11), 112001. doi: <https://doi.org/10.1088/0957-0233/21/11/112001>
31. Darbar, R., Sen, P. Kr., Dash, P., Samanta, D. (2016). Using Hall Effect Sensors for 3D Space Text Entry on Smartwatches. *Procedia Computer Science*, 84, 79–85. doi: <https://doi.org/10.1016/j.procs.2016.04.069>
32. Bolshakova, I. A., Kulikov, S. A., Konopleva, R. F., Chekanov, V. A., Vasilevskii, I. S., Shurygin, F. M. et al. (2014). Application of reactor neutrons to the investigation of the radiation resistance of semiconductor materials of Group III–V and sensors. *Physics of the Solid State*, 56 (1), 157–160. doi: <https://doi.org/10.1134/s1063783414010089>
33. Claes, C., Simoen, E. (2007). *Germanium-Based Technologies*. Oxford: Elsevir. doi: <https://doi.org/10.1016/b978-0-08-044953-1.x5000-5>
34. Udovyt'ska, Yu. A., Luniov, S. V., Kashytskyi, V. P., Maslyuk, V. T., Megela, I. G. (2019). Development of protective coatings based on epoxy composite materials for germanium single crystals from the influence of magnetic field and radiation. *Sensor Electronics and Microsystem Technologies*, 16 (4), 53–65. doi: <https://doi.org/10.18524/1815-7459.2019.4.178074>
35. Babich, V. M., Baranskii, P. I., Shershel, V. A. (1970). The influence of oxygen and impurity-oxygen complexes on magnetoresistance of N-Ge in strong magnetic fields. *Physica Status Solidi (b)*, 42 (1), K23–K27. doi: <https://doi.org/10.1002/pssb.19700420152>
36. Zhang, S., Zhao, D. (2017). *Advances in magnetic materials: processing, properties, and performance*. CRC press. doi: <https://doi.org/10.4324/9781315371573>